Chemosphere 229 (2019) 374–382

Contents lists available at ScienceDirect

Chemosphere

journal homepage: www.elsevier.com/locate/chemosphere

Chlorine incorporation into dye degradation by-product (coumarin) in UV/peroxymonosulfate process: A negative case of end-of-pipe treatment

Ying Huang [a], Bo Sheng [a], Fei Yang [a], Zhaohui Wang [a, b, c, *], Yizhen Tang [d], Qingze Liu [a], Xiaoxiao Wang [a], Jianshe Liu [a, e]

[a] State Environmental Protection Engineering Center for Pollution Treatment and Control in Textile Industry, College of Environmental Science and Engineering, Donghua University, Shanghai, 201620, China
[b] School of Ecological and Environmental Sciences, Shanghai Key Laboratory for Urban Ecological Process and Eco-Restoration, East China Normal University, Shanghai, 200241, China
[c] Institute of Eco-Chongming (IEC), Shanghai, 200062, China
[d] School of Environmental and Municipal Engineering, Qingdao University of Technology, Fushun Road 11, 266033, Qingdao, China
[e] Shanghai Institute of Pollution Control and Ecological Security, Shanghai, 200092, China

HIGHLIGHTS

- A dual effect of Cl^- on coumarin degradation in UV/PMS systems was observed.
- AOX value increased markedly with the addition of chloride.
- Some toxic chlorinated byproducts were identified by GC-MS measurement.
- Mineralization rate of coumarin decreased with increasing Cl^-.
- Effective measures should be taken to mitigate the adverse effect of chloride.

ARTICLE INFO

Article history:
Received 13 January 2019
Received in revised form
30 April 2019
Accepted 3 May 2019
Available online 4 May 2019

Handling Editor: Xiangru Zhang

Keywords:
Sulfate radicals
Fluorescent probe
Chlorinated byproducts
Saline wastewater
Acute toxicity

ABSTRACT

Recently, UV/peroxymonosulfate (PMS) seems as a panacea for the treatment of recalcitrant organic pollutants; however, the presence of high concentration of chloride in saline wastewater indeed complicates this end-of-pipe technology. Here a negative case of UV/PMS for the treatment of one of secondary degradation byproducts of dyes (coumarin, COU) is demonstrated. The removal rate of COU is reduced by addition of Cl^- (0–10 mM). Further increase in Cl^- content favors a rapid COU degradation, whereas Cl^- involvement seems to open a "Pandora's box": 1) a variety of chlorinated organic intermediates such as 4-chloroisocoumarin and 5-chloro-2-hydroxy-benzaldehyde are identified; 2) Accumulation and relative increase of absorbable organic halogen (AOX) with reaction time in the presence of high levels of chloride are observed; 3) the acute toxicity of the treated COU solution increases; 4) mineralization rate of COU decreases with the increasing $[Cl^-]$. The fluorescence intensity in the UV/PMS/COU system declines with the addition of Cl^-, implying the scavenging effects of chloride on hydroxyl radicals. The possible reaction pathways of COU are discussed. These findings highlight the imperativeness of minimizing auxiliary salt dosages in dyeing processes (i.e., source reduction) and developing new end-of-pipe technologies that can work in a saline environment.

© 2019 Elsevier Ltd. All rights reserved.

1. Introduction

Advanced oxidation processes (AOPs), especially ultraviolet (UV)-based AOPs, have proved to be effective in the degradation of recalcitrant organic pollutants (Deng et al., 2013; He et al., 2013; Khan et al., 2013). UV-photolyzed peroxymonosulfate (PMS), an

* Corresponding author. State Environmental Protection Engineering Center for Pollution Treatment and Control in Textile Industry, College of Environmental Science and Engineering, Donghua University, Shanghai, 201620, China.
E-mail address: zhwang@des.ecnu.edu.cn (Z. Wang).

https://doi.org/10.1016/j.chemosphere.2019.05.024
0045-6535/© 2019 Elsevier Ltd. All rights reserved.

efficient precursor of $SO_4^{\bullet-}$ production, is suggested to generate $^{\bullet}OH$ and $SO_4^{\bullet-}$ in a benign and economic way (Guan et al., 2010; Verma et al., 2016). However, recent investigations indicate that chloride ions in chloride-rich wastewater would greatly influence the oxidation efficiency of AOPs by scavenging radicals (e.g., $SO_4^{\bullet-}$ or $^{\bullet}OH$) to yield less reactive chlorine radicals ($Cl_2^{\bullet-}$/$Cl^{\bullet}$) or reacting directly with PMS to produce Cl_2/HClO (Wang et al., 2011a, 2017a; Fang et al., 2016). Wang et al. (2011a) reported that the decolorization rate of acid orange 7 (AO7) was inhibited when $[Cl^-] < 0.1$ M, whereas it accelerated with increase in Cl^- dosage up to 1.0 M in the UV/PMS system. However, our recent work indicated that absorbable organic halogen (AOX) and even some more toxic organic byproducts were formed with external chloride by the UV/PMS process (Wang et al., 2017b).

Coumarin (COU), consisting of fused benzene and α-pyrone rings, is an important low-molecular-weight phenolic compound present in natural organic matter, typically found in water (Clark et al., 2002; Leenheer and Croua, 2003). Recently, COU and its derivatives are widely used as antibacterial agents (El-Saghier and Khodairy, 2000), novel dyes (Yıldırım et al., 2016), fluorescent probes, sensors and switches (Donovalová et al., 2012), and so on. In addition, COU is a well-known trapping reagent that could react directly with hydroxyl radicals to generate the strong fluorescent compound 7-hydroxycoumarin (7-HC) (Liu et al., 2017; Zhang and Nosaka, 2013; Ikhlaq et al., 2012; Jean-M et al., 2018) (shown in eq. (1)). Newton and Milligan (2006) reported that the yield of 7-HC formation in their radiolysis experiments is estimated as 4.7% per generated $^{\bullet}OH$. The fraction of $^{\bullet}OH$ not resulting in 7-HC would produce other nonfluorescent hydroxylated compounds, which is not detected by the technique used (Burgos-Castillo et al., 2018; Newton and Milligan, 2006; Louit et al., 2005). Therefore, 7-HC is supposed to be a reliable indicator of $^{\bullet}OH$ attack.

$$\text{Coumarin} + {}^{\bullet}OH \rightarrow \text{7-HC},\ k = 5.6 \times 10^9\ M^{-1}\ s^{-1} \quad (1)$$

Recently, our investigations demonstrated that the impacts of chloride on the oxidation of dyes and their intermediate (phthalic acid) were substantially different (Huang et al., 2017). Interestingly, COU is also one of the degradation intermediates of dyes in AOPs (Stylidi et al., 2003; Wang et al., 2014; Yuan et al., 2011, 2012; Tao et al., 2015; Huang et al., 2018a). COU could be produced during the degradation of AO7 in the UV/TiO_2 system (Stylidi et al., 2003; Wang et al., 2014; Yuan et al., 2012), Co/PMS system (Yuan et al., 2011), and PI (polyimides)/PMS/Vis system (Tao et al., 2015). Yuan et al. (2012) observed that further degradation of coumarin would generate heterocyclic compounds containing a five- and a six-atom ring, such as 1(3H)-isobenzofuranone, 2,3-dihydro-1H-inden-1-one and 1H-indene-1,3(2H)-dione. Moreover, COU was also identified during the decoloration of other azo dyes. Huang et al. (2018a) reported that coumarin was one of the aromatic intermediates of orange G (OG) in activated carbon fiber/ultrasound/peroxydisulfate (ACF/US/PDS) system and would be further oxidized to heterocyclic compounds. However, our previous work have measured some chlorinated coumarin derivatives such as 3,4-dichloroisocoumain (Yuan et al., 2011) and 5-chloro-1-indanone (Yuan et al., 2012). To date, although it is known that the presence of external chloride ions could reduce the formation of 7-HC by competing with COU for reaction with $^{\bullet}OH$ (Lin et al., 2015), the mechanism of formation of chlorinated COU byproducts is largely unknown in AOP-based saline wastewater treatment.

In this study, coumarin is chosen as a typical aromatic intermediate of dyes to examine the degradation kinetics and byproduct generation in the UV/PMS process in the presence and absence of chloride ions. The effects of PMS dosage, pH, and chloride concentration were investigated. Additionally, identification of chlorinated compounds, AOX determination, toxicity analysis, mineralization, and fluorescence intensity measurement were carried out. A possible oxidation pathway is proposed. These results may provide valuable insight into the degradation mechanism of fluorescent secondary degradation byproducts of dyes and the generation pathway of chlorinated intermediates in the treatment of saline wastewater.

2. Experimental

2.1. Materials

Coumarin ($C_9H_6O_2$, 98%, COU) and Oxone® ([$2KHSO_5 \cdot KHSO_4 \cdot K_2SO_4$] salt, 95%, PMS) of the purest grade available were obtained from Sigma-Aldrich. The chemical structure of COU is shown in Table S1. Na_2SO_3 and $NaNO_2$ were purchased from Sinopharm Chemical Reagent Co., Ltd, China. All the other reagents such as NaCl, NaOH, and H_2SO_4 were of analytical grade and used without further purification. Each stock solution was prepared by Barnstead UltraPure water (18.3 MΩ cm) freshly.

2.2. Procedure

The photodegradation of COU was carried out in an XPA-7-type photochemical reactor (Xujiang Electromechanical Plant, Nanjing, China). A 100 W medium-pressure mercury vapor lamp was used as the light source in a water-cooled borosilicate glass immersion well. The light intensity at reactor vessel positions was measured to be 12.7 mW/cm^2 by a UV-A irradiation meter supplied by Photoelectric Instrument Factory of Beijing Normal University, China. The spectrum distribution and relative energy of the Hg lamp are shown in Table S2. An open borosilicate glass quartz tube of 50 ml capacity at a batch mode was used for all the photodegradation experiments at room temperature without controlling the pH unless specified. Samples were taken from the solution at specific time intervals and quenched with $NaNO_2$ for GC-MS, TOC, AOX, or toxicity analysis immediately. Each experiment was performed in duplicate, with the final data error less than 5%.

2.3. Analysis

The concentration of COU was measured on a UV–Vis spectrophotometer (Hitachi Model U-2910) at 277 nm, as recommended by Ikhlaq et al. (2012). The calibration curve for COU is shown in Fig. S2 ($R^2 = 0.998$), with the limit of detection as 0.06 ppm. AOX was determined using an instrumental analyzer (AOX, multi X 2500, Jena, Germany). Samples were adjusted to pH < 2.0 before enrichment on activated carbon. The Automatic Preparation Unit 2 (Jena, Germany) for automatic sample adsorption was used for pretreating samples. The temperature of the combustion system was set to 950 °C. HCl (0.010 M) was applied for titration. The detection limit of AOX was 1 μg (calculated as the absolute content of chloride). A multi N/C 3100 TOC analyzer (Jena, Germany) was applied to measure total organic carbon (TOC), with a detection limit of 4.0 μg/L. Owing to the role of COU as a fluorescent probe for $^{\bullet}OH$ generated by UV irradiation (Czili and Horvath, 2008; Du et al., 2008), a luminescence spectrometer (LS55, PerkinElmer precisely) was employed to verify the formation of $^{\bullet}OH$ during the oxidation process. 7-Hydroxycoumarin was measured by monitoring the fluorescence emission at 460 nm under excitation at 332 nm. A bioluminescent bacterium, *Photobacterium phosphoreum* (CS233), was used as the indicator for toxicity analysis on a toxicity testing instrument (BHP9514, Hamamatsu Photon Medical Technology (Langfang) Co., Ltd). The bioluminescence was assessed by the relative luminosity and measured after 15 min of exposure at

20 °C.All the samples were tested in duplicate to obtain an average value. To identify the intermediate products during the COU degradation process, a gas chromatography-mass spectrometer (GC-MS) (Agilent 7890A-5975C, USA) was employed. Samples were pretreated by the solid phase extraction (SPE) method (using CNWBOND LC-C18 SPE tube) and silylation method (using hexamethyldisilazane and chlorotrimethylsilane). A gas chromatograph (Agilent 7890A) equipped with a HB-5 MS capillary column (30 m × 320 μm × 0.5 μm film thickness), interfaced directly to the mass spectrometer (5975A inert XL MSD with Triple-Axis Detector), was used to obtain the spectra. The column oven was programmed from 40 °C (2 min) to 100 °C at a rate of 12 °C/min, then to 200 °C at 5 °C/min, and finally to 270 °C (5 min) at a rate of 20 °C/min. Electron impact (EI) mode at 70 eV was used, and the spectra were obtained in a scan range of 10–400 *m/z*. Analysis of the intermediates was verified from the NIST08 mass spectral library database.

The pseudo-first-order kinetic model was adopted to describe the degradation kinetics under various oxidation conditions, and the expression is shown in eq. (2), where C_0 and C represent COU concentrations (mM) at time t = 0 and t min, respectively; *k* is the observed pseudo-first-order rate constant (min^{-1}); and t represents the reaction time (min).

$$C / C_0 = e^{-kt} \quad (2)$$

Relative luminosity is regarded as one of the most common analytical indexes in bacterium toxicity testing, as shown in eq. (3) (Zhao et al., 2015), where I_i and I_0 are the luminous intensities (a.u.) of the COU sample and standard sample (3% NaCl), respectively.

$$\text{Relative luminosity}(\%) = I_i / I_0 \times 100\% \quad (3)$$

3. Results and discussion

3.1. COU degradation

3.1.1. Effect of peroxymonosulfate concentration

The impact of peroxymonosulfate concentration on COU degradation rates in the UV/PMS system was investigated. As illustrated in Fig. 1a, an increase in the PMS level resulted in faster oxidation of COU. The degradation rate constant increased from 2.33×10^{-3} to 9.57×10^{-2} min^{-1} ($R^2 > 0.98$), while the content of PMS varied from 0 to 10 mM. The formation of free radicals from UV-assisted PMS activation is supposed to increase with PMS dosage, hence leading to the decomposition of the substrate efficiently. Notably, 18% of COU was degraded with 0 mM PMS after 90 min treatment, possibly due to the photocleavage of coumarin under UV irradiation (Fan et al., 2014). Czili and Horvath, 2008 also demonstrated that a slow degradation of COU occurred and a small amount of luminescent compounds were generated by exposing COU to UV light (40 W).

3.1.2. Effect of pH

It is suggested that pH is a significant parameter in the treatment of wastewater based on AOPs (Guan et al., 2010; Sheng et al., 2018). Fig. 1b presents the impact of the initial solution pH on the oxidation of coumarin. The kinetic rate constant (*k*) ranged from 3.1×10^{-2} to 3.4×10^{-2} min^{-1} at pH 2.0–7.0. This indicates that UV/PMS is not significantly affected by the change in pH. Khan et al. (2014) also reported that the performance of UV/PMS was more independent of initial pH values when they determined the degradation of atrazine by UV/peroxygen. The pH independence of degradation efficiency of UV/PMS probably resulted from the unchanged radical quantum yield while the solution pH was less than 8.0 (Guan et al., 2010).

3.1.3. Effect of Cl^- concentration

It is well known that chloride ions would affect the efficiency of AOPs considerably (Liao et al., 2001; De Laat and Le, 2006). Therefore, the impact of different concentrations of chloride ions on the COU degradation process was investigated. As displayed in Fig. 1c, a dual effect of Cl^- with a different concentration on the COU oxidation process was observed. An inhibitory impact occurred at a low Cl^- content (<10 mM), whereas an accelerating impact of Cl^- was found when [Cl^-]>10 mM. Moreover, the higher concentrations of chloride ions strongly enhanced the degradation rates of COU. This phenomenon was also observed in the oxidation of dyes and other organic contaminants (Wang et al., 2017b; Wang et al., 2011a,b; Zhou et al., 2015). Wang et al. (2011a,b) found that chloride played a dual (inhibitory, then promoting) impact on Org II dye bleaching in the Co^{2+}/PMS system. A similar phenomenon was also discovered on the oxidation process of 4-chlorophenol (Wang et al., 2017b) and 4-chloro-2-nitrophenol (Zhou et al., 2015) in PMS-based systems.

3.2. AOX formation

Various degradation intermediates, potentially more toxic than their parent organic compound, would occur during the application of AOPs (Xu et al., 2013; Qi et al., 2014; Karci et al., 2012). AOX is a significant variable for the identification of halogenated compounds and would provide more overall information about the impact of Cl^- on efficiencies of AOPs. As shown in Fig. 1d, AOX formation during COU oxidation with different chloride contents in the UV/PMS system was investigated. The formation of AOX was found to be a time-dependent process, and AOX accumulated gradually within 90 min of reaction. The value of AOX increased rapidly when Cl^- dosage increased from 0 to 100 mM. It is worth noting that the AOX value exceeded the current German AOX threshold value for wastewater (0.5 mg/L) when the Cl^- content was up to 50 mM. Therefore, the secondary degradation products of dyes are likely to form more toxic organic pollutants in saline wastewater once they are discharged into the environment without further treatment.

3.3. Fluorescence intensity measurement

To further investigate the formation and transformation of radicals during the reaction, the intensity of fluorescence was measured (Fig. 2). The fluorescence intensity is not necessarily correlated with the reaction time in the UV/PMS system. The maximum fluorescence intensity occurred at 5 min, whereas the fluorescence intensity decreased significantly afterwards. The degradation of COU at different Cl^- dosages (0–300 mM) with pH varying from 2.0 to 7.0 was further studied. As shown in Fig. 3 and Fig. S3, the maximum fluorescence intensity reduced significantly by increasing the initial chloride levels at the same pH value. For example, the maximum fluorescence intensity in the absence of chloride was 17 times higher than that in the presence of 300 mM chloride at pH = 3.0. This indicates that the formation of 7-HC decreases with increase in initial contents of chloride. Moreover, as shown in Fig. 3, the maximum fluorescence intensity was considerably enhanced with pH increasing from 2.0 to 7.0 at the same chloride dosage, which indicates an increase in 7-HC production. Therefore, the yield of $^{\bullet}OH$ trapped by COU was dependent on the reaction time, chloride levels, and pH.

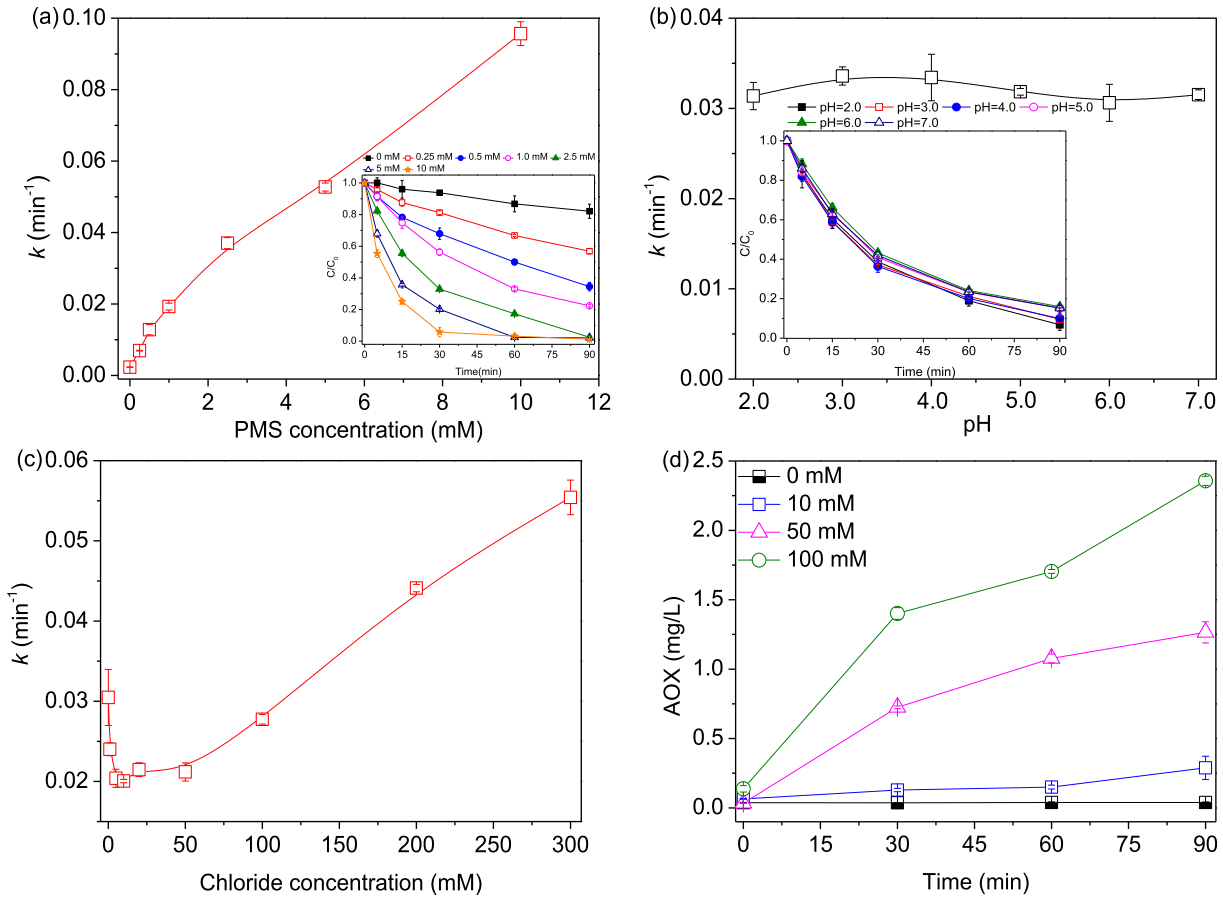

Fig. 1. Effect of PMS concentration (a), pH (b), and chloride (c) concentration on coumarin degradation rates and AOX formation (d) with different concentrations of chloride during UV/PMS treatment. Conditions: $[coumarin]_0 = 0.1$ mM, $[PMS]_0 = 2.5$ mM, pH = 3.0 (except for Fig. 1(b)), temperature = 25 °C.

3.4. Identification of intermediates

GC-MS was applied to identify the intermediates produced in the oxidation of COU for the two Cl^- contents (i.e., 10 and 100 mM) during 90 min of reaction time. Thirteen kinds of aromatic intermediates were detected in the presence of 10 mM chloride in the solution, such as benzofuranone, benzaldehyde, benzoic acids, phenols (Miller et al., 1975), and so on, whereas no chlorinated intermediates were identified in the solution. However, when the Cl^- dosage was increased up to 100 mM, 19 kinds of aromatic products (e.g., benzofuran and phenols (Miller et al., 1975)) and 8 chlorinated organic byproducts were identified in the reaction solution.

To confirm the position of Cl atom in the chlorinated compounds, the NBO (natural bond orbital) charge population of the carbon cation was calculated approximately by employing quantum chemistry methods at the B3LYP/6-311 + G** levels of theory (Frisch et al., 2009). As shown in Fig. 4, the NBO charge for the C1 and C2 atoms was 0.519 and −0.165 e, respectively, which indicates the C1 atom easily loses electrons compared to the C2 atom, and $Cl_2^{\bullet-}$ radical is more feasible to react with C1 than with C2. Two possible products, P1 (4-chloroisocoumarin) and P2 (3-chloroisocoumarin), are illustrated in Fig. 4. P2 was approximately 10 kJ/mol lower than P1 at the levels of B3LYP/6-311 + G**. Therefore, it is assumed that P2 (3-chloroisocoumarin) should be the dominant product as COU is chlorinated. In addition, 5-chloro-2-hydroxy-benzaldehyde, tetrahydrofurfuryl chloride, 3-chloropropionic acid tetrahydro-furan-2-ylmethyl ester, and other small molecular chlorinated products were identified with 100 mM chloride in the reaction, as illustrated in Fig. 5. Hence, the number of identified intermediates, especially chlorinated byproducts, is enhanced with an increase in Cl^- dosages during the reaction process.

To further identify the generation and transformation of chlorinated organic products with reaction time in the UV/PMS system, a variety of intermediate products at 30 min, 60 min, and 90 min were analyzed, as listed in Table S3. It indicates that the chlorinated byproducts could be detected at the beginning of the reaction and were accumulated with time. Moreover, a highly fluorescent compound, 7-hydroxycoumarin (7-HC), was detected only at low levels of Cl^- dosages (10 mM). This could be attributed to the reason that excess Cl^- could compete with COU for $^{\bullet}OH$ in the solution with a high reaction rate (Buxton et al., 1988) at high Cl^- concentration.

3.5. Toxicity

Toxicity was assessed for samples collected initially and at 90 min of reaction time using luminous bacteria. Table S4 shows the potential toxic effect of degradation byproducts by monitoring the luminosity change of COU in the presence of Cl^- in the UV/PMS system. The relative luminosity intensity of blank control containing only 3% NaCl was 100.7% and 100.6% at 0 and 90 min, respectively. In UV/PMS (without Cl^-), the relative luminosity intensity of the initial COU solution was 99.8%, which decreased to 93.8% after reaction for 90 min. In the presence of 10 mM chloride, the relative luminosity intensity decreased from 98.4% to 91.6% after 90 min of

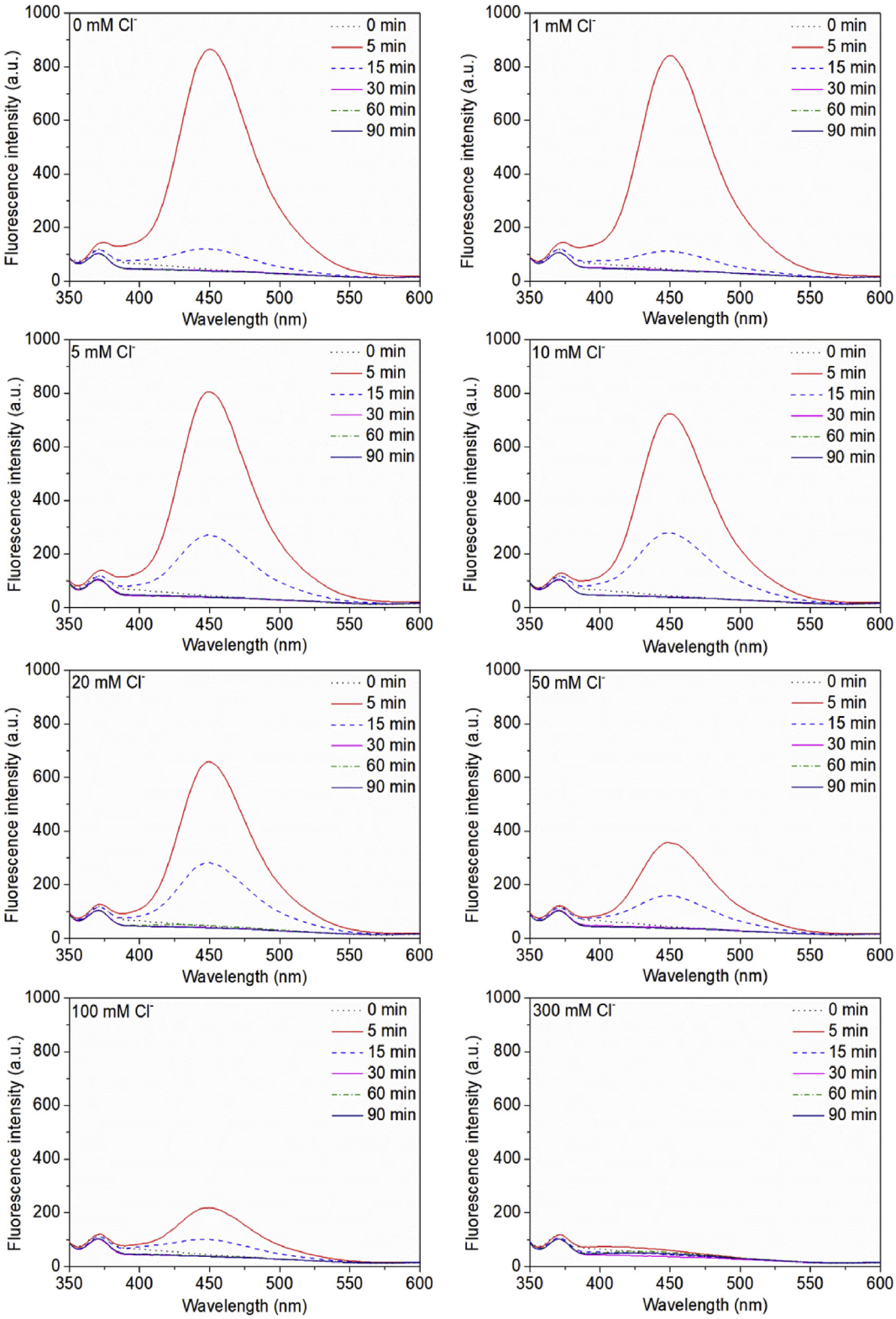

Fig. 2. Fluorescence intensity of the coumarin degradation process during UV/PMS treatment in the presence of different Cl^- concentrations. Condition: $[coumarin]_0 = 0.1$ mM, $[PMS]_0 = 2.5$ mM, pH = 3.0, temperature = 25 °C.

oxidation. When the Cl^- concentration was up to 100 mM, the relative luminosity intensity changed from 97.2% to 89.8% after 90 min of treatment. The results clearly indicate that the acute toxicity of the COU solution increases as both Cl^- dosages and reaction time increase, which is in good agreement with the data from GC-MS and AOX measurement. There have been some examples where the parent compound is less toxic than degradation products such as 4-chloro-2-methylphenoxyacetic acid (Zertal

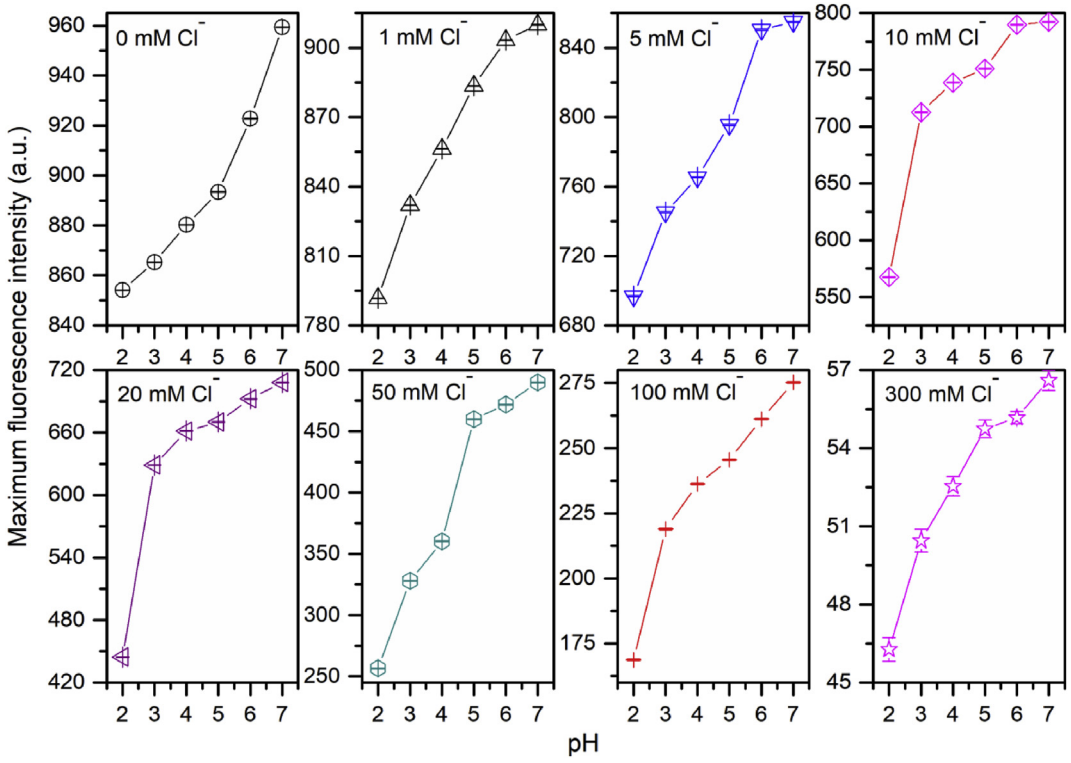

Fig. 3. Effect of chloride contents on maximum fluorescence intensity at different pH values during the coumarin degradation process in the UV/PMS system. Condition: $[coumarin]_0 = 0.1$ mM, $[PMS]_0 = 2.5$ mM, time = 5 min, temperature = 25 °C.

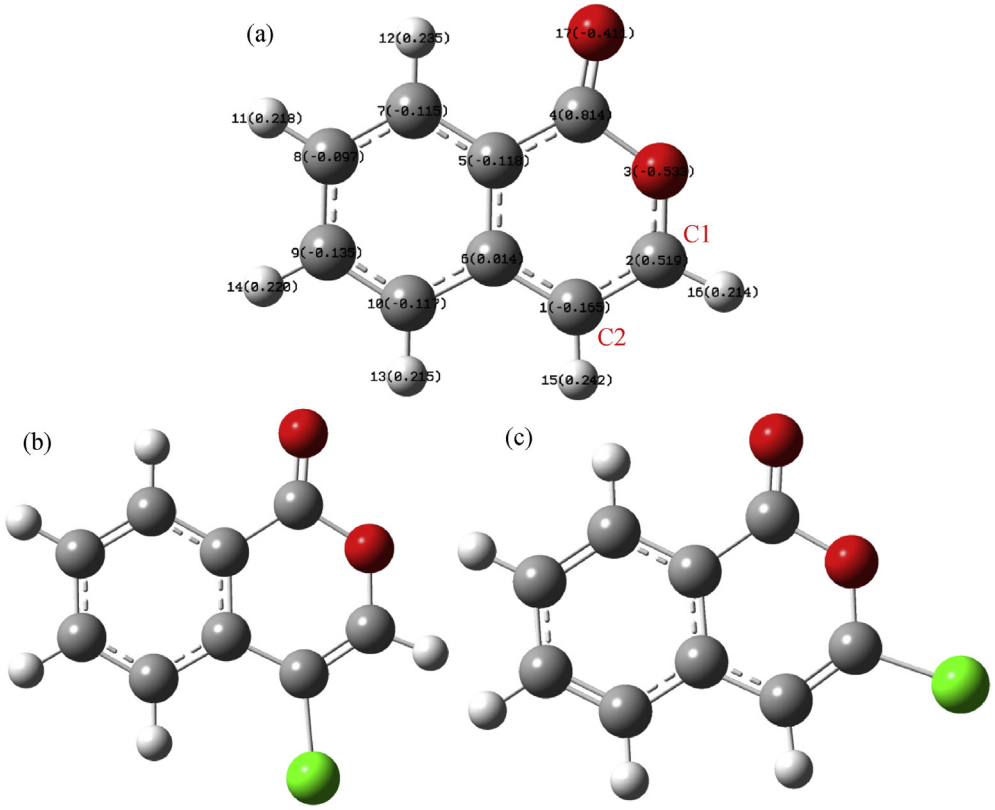

Fig. 4. Optimized geometric structure and mulliken atomic charges of coumarin radical cation (a) and its possible byproducts P1 (b) and P2 (c) after reaction with $Cl_2^{\bullet-}$. Gray, red, green, and white represent carbon, oxygen, chlorine, and hydrogen, respectively. (For interpretation of the references to color in this figure legend, the reader is referred to the Web version of this article.)

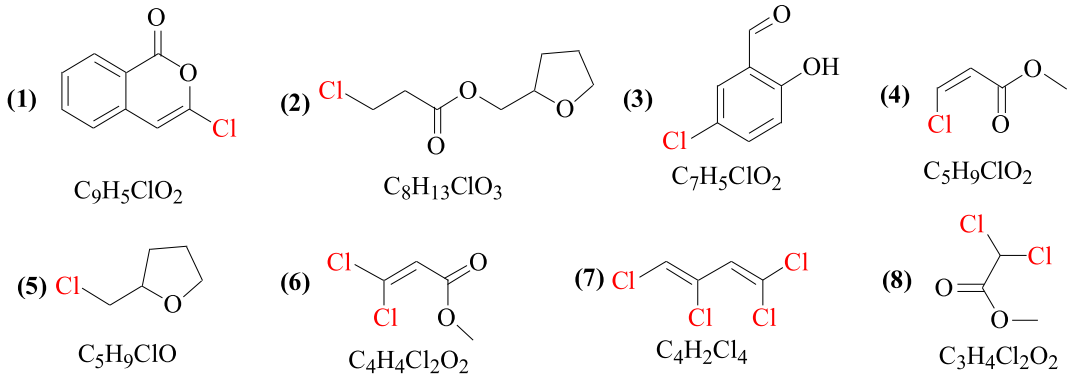

Fig. 5. Identification of chlorinated byproducts in the coumarin degradation process with 100 mM chloride ion in the UV/PMS system. Condition: $[coumarin]_0 = 0.1$ mM, $[PMS]_0 = 2.5$ mM, pH = 3.0, temperature = 25 °C.

et al., 2001), 2,4,6-trichlorophenol (Fang et al., 2016), and 4-chlorophenol (Wang et al., 2017b).

3.6. Mineralization

AOX measurement, GC-MS analysis, and toxicity test all indicate that chlorinated organic products would be formed when certain contents of chloride are present in the UV/PMS system. Hence, it is necessary to measure TOC values in addition to degradation rates to evaluate the oxidation efficiencies of the UV/PMS/Cl^- system. As depicted in Fig. 6, the mineralization percentage of COU increased when the reaction time extended. TOC removal of COU without chloride addition was 16.3%, 29.9%, and 34.8% after 30 min, 60 min, and 90 min of the reaction, respectively. However, in the presence of chloride ion (10–100 mM), the extent of mineralization decreased with increase in Cl^- contents. Only 13.3% of COU was mineralized in the presence of 100 mM Cl^- after 90 min of oxidation. A similar phenomenon (high degradation rate but low mineralization extent) was observed with the oxidation of the dye AO7 by Yuan et al. (2011). Moreover, the effect of pH on the mineralization of COU was further investigated, as shown in Fig. S4. It indicates that the mineralization of COU was nearly independent of pH.

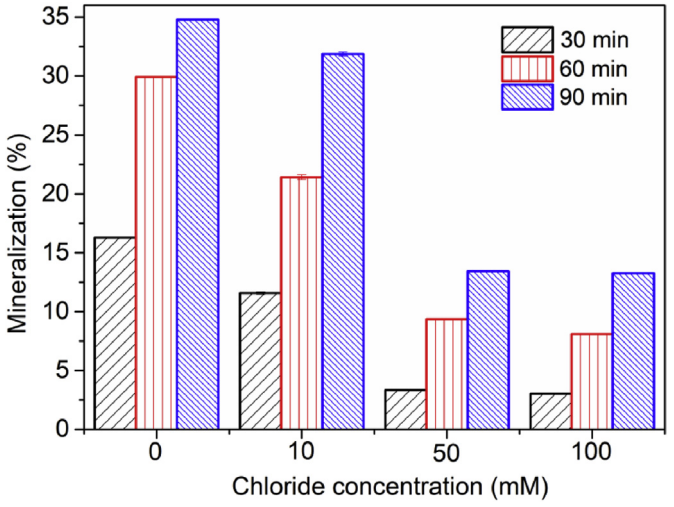

Fig. 6. Mineralization of coumarin degradation with different concentrations of chloride in the UV/PMS system. Condition: $[coumarin]_0 = 0.1$ mM, $[PMS]_0 = 2.5$ mM, pH = 3.0, temperature = 25 °C.

3.7. Proposed reaction mechanism

According to the kinetic data and degradation intermediates identified by GC-MS and in previous studies (Huang et al., 2017; Wang et al., 2011b, 2017b), a possible reaction mechanism is proposed for the production of chlorinated organic byproducts during the degradation of coumarin in the UV/PMS system.

It is suggested that $SO_4^{\bullet-}$ generated by a one-electron process from PMS reduction would be further scavenged by Cl^- in the solution to form less reactive chlorine radicals ($Cl^{\bullet}/Cl_2^{\bullet-}$). This set of reactions would lead to the reduction of COU degradation. This inhibiting impact of chloride ion is significant at low dosages of chloride (<10 mM). Hence, the mineralization rate of COU decreases. Moreover, it reported that $SO_4^{\bullet-}$ could be converted to $^{\bullet}OH$ (Lutze et al., 2015), especially in a weakly acidic or neutral solution (Guan et al., 2010). However, $SO_4^{\bullet-}$ could be quenched by additional Cl^-, leading to the reduced yield of $^{\bullet}OH$ in the aqueous solution. Therefore, the fluorescence intensity decreased.

A further addition of chloride ion dramatically increased the COU degradation. Chloride ions are directly oxidized by PMS through two-electron transfer (eq (4) and (5)) to yield active chlorine species ($HOCl/Cl_2$) (Lente et al., 2009), which could rapidly decompose COU. These reactions would govern the overall COU degradation with high contents of chloride (>10 mM). However, some refractory chlorinated organic compounds with aromatic ring were detected by GC-MS with the increase in Cl^- content, which decrease the mineralization degree of COU and increase the AOX levels. More importantly, chlorinated byproducts are more toxic than their precursors. In addition, HOCl generated in the presence of high levels of chloride is supposed to quench 7-HC in the reaction solution (Payá et al., 1992) or directly react with COU, but their products are nonfluorescent.

$$2Cl^- + HSO_5^- + H^+ \rightarrow SO_4^{2-} + Cl_2 + H_2O \quad (4)$$

$$Cl^- + HSO_5^- \rightarrow SO_4^{2-} + HOCl \quad (5)$$

Based on the oxidation products identified by GC-MS and the results exhibited in Fig. 5, a possible pathway for COU degradation in the UV/PMS system under a chloride-rich solution is proposed, as shown in Fig. S5. First, the oxidation of COU could form heterocyclic compounds such as benzofuran, 3(2H)-benzofuranone, and 7-hydroxycoumarin. The heterocyclic compounds could be further oxidized to 2-hydroxybenzaldehyde, 2-hydroxybenzoic acid methyl ester, 4-ethyl-benzoic acid methyl ester, 3,4-dimethyl-benzoic acid methyl ester, and phenol. In addition, the partial degradation of the above aromatic organic compounds would

produce carboxylic acids such as 3-(2-hydroxyphenyl)-acrylic acid, 3-hydroxy-3-(4-hydroxyphenyl)-propionic acid, phthalic acid diisobutyl ester, and so on. Some organic acid products and alkanes such as acetic acids, propionic acids, pentanoic acids, butane-1,4-diol, and propane-1,3-diol could be formed in the UV/PMS system. Some ring-opening compounds may be oxidized to CO_2 and H_2O.

It is well known that $Cl^{\bullet}/Cl_2^{\bullet-}$ radicals formed by scavenging $SO_4^{\bullet-}$ radical by Cl^- may react with organic compounds and their intermediate products by H-abstraction, one-electron oxidation, and addition to the unsaturated C—C bonds, which depended on the character of the substrate (Grebel et al., 2010; Hasegawa and Neta, 1978). The formation of the main chlorinated intermediates detected in the system is shown in Fig. S2. First, the $SO_4^{\bullet-}$ radical may add to the aromatic ring of the intermediates of the COU degradation in all cases (Anipsitakis et al., 2006). The formation of the corresponding chlorinated species takes place by electrophilic substitution mostly in the para or ortho position of the aromatic organic compounds (see Fig. S6 for more details).

In our previous work, the degradation of phthalic acid (PA), one of the common degradation byproducts of dyes, and the production of AOX were inhibited with increasing chloride ion levels in the Co/PMS system (Huang et al., 2017) owing to the low reaction activity of the chlorine species toward the aromatic ring with a deactivating carboxyl group on it. This indicates that most of chlorinated organic byproducts formed during the dye oxidation process may root from the chlorination of the parent compounds of PA (dyes or other main intermediates) in chloride-rich waters. Moreover, an inhibitory effect of Cl^- on maleic acid (MA) decomposition was observed in the Fe/PMS system, whereas the yield of AOX increased (Huang et al., 2018b). This could be ascribed to the low reactivity of chlorine towards unsaturated bonds and carboxylic acid moieties. Chlorination of the secondary degradation byproducts of organic compounds rather than MA itself was responsible for the accumulation of the chlorinated byproducts in the presence of Cl^- during dyeing wastewater treatment. However, a dual effect of Cl^- on COU oxidation and the accumulation of AOX by the UV/PMS process indicates that the chlorination of COU itself could possibly lead to the generation of the chlorinated byproducts during dye degradation in a chloride-rich environment. Therefore, the molecular structure of the secondary degradation byproducts of dyes is important for the generation of chlorinated byproducts in industrial chloride-rich wastewater. The presence of deactivating groups is supposed to reduce the degradation of substrates and affect the formation pathway of AOX.

4. Conclusions

The effect of chloride on the UV/PMS oxidation process of COU was tested in this study. A dual (inhibitory, then accelerating) effect of Cl^- levels (0–300 mM) on COU depletion was observed, while the mineralization of COU reduced by enhancing the chloride contents. The formation of potentially more toxic chlorinated organic compounds was identified by GC-MS in the presence of chloride, which was confirmed by the results of AOX accumulation and acute toxicity measurement. The decrease in fluorescence intensity of the reaction solution with increase in Cl^- dosage indicates transformation of $^{\bullet}OH$ to other oxidized species and/or decay of COU or 7-HC as a result of radicals or reactive chlorine attack. However, the conversion efficiency from $SO_4^{\bullet-}$ to $^{\bullet}OH$ dramatically enhanced with the degradation rate of COU unchanged when pH increased from 2.0 to 7.0. Thus, a possible reaction pathway was proposed. Hence, UV/PMS may be not suitable for the treatment of saline wastewater because of low mineralization rate, elevated toxicity, and toxic byproduct formation in the presence of chloride. It is imperative to develop a new end-of-pipe technology for the treatment of secondary degradation intermediates of recalcitrant organic compounds.

Acknowledgments

This work was supported by National Key Research and Development Program of China (2016YFC0400501/2016YFC0400509), National Natural Science Foundation of China (No. 21677031 and 41775119), and the Fundamental Research Funds for the Central Universities (CUSF-DH-D-2017095). Z.H.W would like to thank the support of State Key Laboratory of Pollution Control and Resource Reuse Fund (PCRRF16006).

Appendix A. Supplementary data

Supplementary data to this article can be found online at https://doi.org/10.1016/j.chemosphere.2019.05.024.

References

Anipsitakis, G.P., Dionysiou, D.D., Gonzalez, M.A., 2006. Cobalt-mediated activation of peroxymonosulfate and sulfate radical attack on phenolic compounds. Implications of chloride ions. Environ. Sci. Technol. 40, 1000–1007. https://doi.org/10.1021/es050634b.

Buxton, G.V., Greenstock, C.L., Helman, W.P., Ross, A.B., 1988. Critical review of rate constants for reactions of hydrated electrons, hydrogen atoms and hydroxyl radicals ($^{\bullet}OH/^{\bullet}O^-$) in aqueous solution. J. Phys. Chem. Ref. Data 17 513–886. https://doi.org/10.1063/1.555805.

Burgos-Castillo, R.C., Jean-M, F., Xochitl, D.B., Mika, S., 2018. Towards reliable quantification of hydroxyl radicals in the Fenton reaction using chemical probes. RSC Adv. 8, 5321–5330. https://doi.org/10.1039/C7RA13209C.

Clark, D., Jimenez-Morais, J., Jones, G., Zanardi-Lamardo, E., Moore, C.A., Zika, R.G., 2002. A time-resolved fluorescence study of dissolved organic matter in a riverine to marine transition zone. Mar. Chem. 78, 121–135. https://doi.org/10.1016/S0304-4203(02)00014-2.

Czili, H., Horváth, A., 2008. Applicability of coumarin for detecting and measuring hydroxyl radicals generated by photoexcitation of TiO_2 nanoparticles. Appl. Catal. B Environ. 81, 295–302. https://doi.org/10.1016/j.apcatb.2008.01.001.

De Laat, J., Le, T.G., 2006. Effects of chloride ions on the iron(III)-catalyzed decomposition of hydrogen peroxide and on the efficiency of the Fenton-like oxidation process. Appl. Catal. B Environ. 66, 137–146. https://doi.org/10.1016/j.apcatb.2006.03.008.

Deng, J., Shao, Y.S., Gao, N.Y., Xia, S.J., Tan, C.Q., Zhou, S.Q., Hu, X.H., 2013. Degradation of the antiepileptic drug carbamazepine upon different UV-based advanced oxidation processes in water. Chem. Eng. J. 222, 150–158. https://doi.org/10.1016/j.cej.2013.02.045.

Donovalová, J., Cigáň, M., Stankovičová, H., Gašpar, J., Danko, M., Gáplovský, A., Hrdlovič, P., 2012. Spectral properties of substituted coumarins in solution and polymer matrices. Molecules 17, 3259–3276. https://doi.org/10.3390/molecules17033259.

Du, L.P., Li, M.Y., Zheng, S.L., Wang, B.H., 2008. Rational design of a fluorescent hydrogen peroxide probe based on the umbelliferone fluorophore. Tetrahedron Lett. 49, 3045–3048. https://doi.org/10.1016/j.tetlet.2008.03.063.

El-Saghier, A.M.M., Khodairy, A., 2000. New synthetic approaches to condensed and spiro coumarins: coumarin-3-thiocarboxamide as building block for the synthesis of condensed and spiro coumarins. Phosphorus Sulfur 160, 105–119. https://doi.org/10.1080/10426500008043675.

Fan, W.Z., Tong, X., Yan, Q., Fu, S.Y., Zhao, Y., 2014. Photodegradable and size-tunable single-chain nanoparticles prepared from a single main-chain coumarin-containing polymer precursor. Chem. Commun. 50, 13492–13494. https://doi.org/10.1039/C4CC06629D.

Fang, C.L., Xiao, D.X., Liu, W.Q., Lou, X.Y., Zhou, J., Wang, Z.H., Liu, J.S., 2016. Enhanced AOX accumulation and aquatic toxicity during 2,4,6-trichlorophenol degradation in a Co(II)/peroxymonosulfate/Cl^- system. Chemosphere 144, 2415–2420. https://doi.org/10.1016/j.chemosphere.2015.11.030.

Frisch, M.J., et al., 2009. Gaussian 09, Revision D.01. Gaussian, Inc., Wallingford, CT.

Grebel, J.E., Pignatello, J.J., Mitch, W.A., 2010. Effect of halide ions and carbonates on organic contaminant degradation by hydroxyl radical-based advanced oxidation processes in saline waters. Environ. Sci. Technol. 44, 6822–6828. https://doi.org/10.1021/es1010225.

Guan, Y.H., Ma, J., Li, X.C., Fang, J.Y., Chen, L.W., 2010. Influence of pH on the formation of sulfate and hydroxyl radicals in the UV/peroxymonosulfate system. Environ. Sci. Technol. 45, 9308–9314. https://doi.org/10.1021/es2017363.

Hasegawa, K., Neta, P., 1978. Rate constants and mechanisms of reactions of $Cl_2^{\bullet-}$ radicals. J. Phys. Chem. 82, 854–857. https://doi.org/10.1021/j100497a003.

He, X.X., de la Cruz, A.A., Dionysiou, D.D., 2013. Destruction of cyanobacterial toxin cylindrospermopsin by hydroxyl radicals and sulfate radicals using UV-254 nm

activation of hydrogen peroxide, persulfate and peroxymonosulfate. J. Photochem. Photobiol., A 251, 160–166. https://doi.org/10.1016/j.jphotochem.2012.09.017.

Huang, Y., Wang, Z.H., Liu, Q.Z., Wang, X.X., Yuan, Z.J., Liu, J.S., 2017. Effects of chloride on PMS-based pollutant degradation: a substantial discrepancy between dyes and their common decomposition intermediate (phthalic acid). Chemosphere 187, 338–346. https://doi.org/10.1016/j.chemosphere.2017.08.120.

Huang, T.Y., Zhang, K., Qian, Y.J., Fang, C., Chen, J.B., 2018a. Ultrasound enhanced activation of peroxydisulfate by activated carbon fiber for decolorization of azo dye. Environ. Sci. Pollut. Res. 25, 14407–14414. https://doi.org/10.1007/s11356-018-1442-3.

Huang, Y., Sheng, B., Wang, Z.H., Liu, Q.Z., Yuan, R.X., Xiao, D.X., Liu, J.S., 2018b. Deciphering the degradation/chlorination mechanisms of maleic acid in the Fe(II)/peroxymonosulfate process: an often overlooked effect of chloride. Water Res. 145, 453–463. https://doi.org/10.1016/j.watres.2018.08.055.

Ikhlaq, A., Brown, D.R., Kasprzyk-Hordern, B., 2012. Mechanisms of catalytic ozonation on alumina and zeolites in water: formation of hydroxyl radicals. Appl. Catal. B Environ. 123–124, 94–106. https://doi.org/10.1016/j.apcatb.2012.04.015.

Karci, A., Arslan-Alaton, I., Olmez-Hanci, T., Bekbölet, M., 2012. Transformation of 2,4-dichlorophenol by H_2O_2/UV-C, Fenton and photo-Fenton processes: oxidation products and toxicity evolution. J. Photochem. Photobiol., A 230, 65–73. https://doi.org/10.1016/j.jphotochem.2012.01.003.

Khan, J.A., He, X.X., Khan, H.M., Shah, N.S., Dionysiou, D.D., 2013. Oxidative degradation of atrazine in aqueous solution by UV/H_2O_2/Fe^{2+}, UV/$S_2O_8^{2-}$/Fe^{2+} and UV/HSO_5^-/Fe^{2+} processes: a comparative study. Chem. Eng. J. 218, 376–383. https://doi.org/10.1016/j.cej.2012.12.055.

Khan, J.A., He, X., Shah, N.S., Khan, H.M., Hapeshi, E., Fatta-Kassinos, D., Dionysiou, D.D., 2014. Kinetic and mechanism investigation on the photochemical degradation of atrazine with activated H_2O_2, $S_2O_8^{2-}$ and HSO_5^-. Chem. Eng. J. 252, 393–403. https://doi.org/10.1016/j.cej.2014.04.104.

Leenheer, J.A., Croua, J.-P., 2003. Peer reviewed: characterizing aquatic dissolved organic matter. Environ. Sci. Technol. 37, 18–26. https://doi.org/10.1021/es032333c.

Lente, G., Kalmár, J., Baranyai, Z., Kun, A., Kék, I., Bajusz, D., Takács, M., Veres, L., Fábián, I., 2009. One-versus two-electron oxidation with peroxomonosulfate ion: reactions with iron(II), vanadium(IV), halide Ions, and photoreaction with cerium(III). Inorg. Chem. 48, 1763–1773. https://doi.org/10.1021/ic801569k.

Liao, C.H., Kang, S.F., Wu, F.A., 2001. Hydroxyl radical scavenging role of chloride and bicarbonate ions in the H_2O_2/UV process. Chemosphere 44, 1193–1200. https://doi.org/10.1016/S0045-6535(00)00278-2.

Lin, Z.R., Zhao, L., Dong, Y.H., 2015. Quantitative characterization of hydroxyl radical generation in a goethite-catalyzed Fenton-like reaction. Chemosphere 141, 7–12. https://doi.org/10.1016/j.chemosphere.2015.05.066.

Liu, Y.Y., Jin, W., Zhao, Y.P., Zhang, G.S., Zhang, W., 2017. Enhanced catalytic degradation of methylene blue by α-Fe_2O_3/graphene oxide via heterogeneous photo-Fenton reactions. Appl. Catal. B Environ. 206, 642–652. https://doi.org/10.1016/j.apcatb.2017.01.075.

Louit, G., Foley, S., Cabillic, J., Coffigny, H., Taran, F., Valleix, A., Renault, J.P., Pin, S., 2005. The reaction of coumarin with the OH radical revisited: hydroxylation product analysis determined by fluorescence and chromatography. Radiat. Phys. Chem. 72, 119–124. https://doi.org/10.1016/j.radphyschem.2004.09.007.

Lutze, H.V., Kerlin, N., Schmidt, T.C., 2015. Sulfate radical-based water treatment in presence of chloride: formation of chlorate, inter-conversion of sulfate radicals into hydroxyl radicals and influence of bicarbonate. Water Res. 72, 349–360. https://doi.org/10.1016/j.watres.2014.10.006.

Miller, R.W., Sirois, J.C., Morita, H., 1975. The reaction of coumarins with horseradish peroxidase. Plant Physiol 55, 35–41. https://doi.org/10.1104/pp.55.1.35.

Newton, G.L., Milligan, J.R., 2006. Fluorescence detection of hydroxyl radicals. Radiat. Phys. Chem. 75, 473–478. https://doi.org/10.1016/j.radphyschem.2005.10.011.

Payá, M., Halliwell, B., Hoult, J.R.S., 1992. Interactions of a series of coumarins with reactive oxygen species: scavenging of superoxide, hypochlorous acid and hydroxyl radicals. Biochem. Pharmacol. 44, 205–214. https://doi.org/10.1016/0006-2952(92)90002-Z.

Qi, C.D., Liu, X.T., Lin, C.Y., Zhang, X.H., Ma, J., Tan, H.B., Ye, W., 2014. Degradation of sulfamethoxazole by microwave-activated persulfate: kinetics, mechanism and acute toxicity. Chem. Eng. J. 249, 6–14. https://doi.org/10.1016/j.cej.2014.03.086.

Sheng, B., Huang, Y., Wang, Z.H., Yang, F., Ai, L.Y., Liu, J.S., 2018. On peroxymonosulfate-based treatment of saline wastewater: when phosphate and chloride co-exist. RSC Adv. 8, 13865–13870. https://doi.org/10.1039/C8RA00600H.

Stylidi, M., Kondarides, D.I., Verykios, X.E., 2003. Pathways of solar light-induced photocatalytic degradation of azo dyes in aqueous TiO_2 suspensions. Appl. Catal. B Environ. 40, 271–286. https://doi.org/10.1016/S0926-3373(02)00163-7.

Tao, Y.F., Wei, M.Y., Xia, D.S., Xu, A.H., Li, X.X., 2015. Polyimides as metal-free catalysts for organic dye degradation in the presence peroxymonosulfate under visible light irradiation. RSC Adv. 5, 98231–98240. https://doi.org/10.1039/C5RA16532F.

Verma, S., Nakamura, S., Sillanpää, M., 2016. Application of UV-C LED activated PMS for the degradation of anatoxin-a. Chem. Eng. J. 284, 122–129. https://doi.org/10.1016/j.cej.2015.08.095.

Wang, P., Yang, S.Y., Shan, L., Niu, R., Shao, X.T., 2011a. Involvements of chloride ion in decolorization of Acid Orange 7 by activated peroxydisulfate or peroxymonosulfate oxidation. J. Environ. Sci. 23, 1799–1807. http://doi.org/10.1016/S1001-0742(10)60620-1.

Wang, Z.H., Yuan, R.X., Guo, Y.G., Xu, L., Liu, J.S., 2011b. Effects of chloride ions on bleaching of azo dyes by Co^{2+}/oxone regent: kinetic analysis. J. Hazard Mater. 190, 1083–1087. https://doi.org/10.1016/j.jhazmat.2011.04.016.

Wang, Y.S., Shen, J.H., Horng, J.J., 2014. Chromate enhanced visible light driven TiO_2 photocatalytic mechanism on acid orange 7 photodegradation. J. Hazard Mater. 274, 420–427. https://doi.org/10.1016/j.jhazmat.2014.04.042.

Wang, Z.H., Ai, L.Y., Huang, Y., Zhang, J.K., Li, S.T., Chen, J.W., Yang, F., 2017a. Degradation of azo dye with activated peroxygens: when zero-valent iron meets chloride. RSC Adv. 7, 30941–30948. https://doi.org/10.1039/C7RA03872K.

Wang, Z.H., Feng, M., Fang, C.L., Huang, Y., Ai, L.Y., Yang, F., Xue, Y., Liu, W.Q., Liu, J.S., 2017b. Both degradation and AOX accumulation are significantly enhanced in UV/peroxymonosulfate/4-chlorophenol/Cl^- system: two sides of the same coin? RSC Adv. 7, 12318–12321. https://doi.org/10.1039/C7RA01294B.

Xu, L., Yuan, R.X., Guo, Y.G., Xiao, D.X., Cao, Y., Wang, Z.H., Liu, J.S., 2013. Sulfate radical-induced degradation of 2,4,6-trichlorophenol: a de novo formation of chlorinated compounds. Chem. Eng. J. 217, 169–173. https://doi.org/10.1016/j.cej.2012.11.112.

Yuan, R.X., Ramjaun, S.N., Wang, Z.H., Liu, J.S., 2011. Effects of chloride ion on degradation of Acid Orange 7 by sulfate radical-based advanced oxidation process: implications for formation of chlorinated aromatic compounds. J. Hazard Mater. 196, 173–179. https://doi.org/10.1016/j.jhazmat.2011.09.007.

Yuan, R.X., Ramjaun, S.N., Wang, Z.H., Liu, J.S., 2012. Photocatalytic degradation and chlorination of azo dye in saline wastewater: kinetics and AOX formation. Chem. Eng. J. 192, 171–178. https://doi.org/10.1016/j.cej.2012.03.080.

Yıldırım, F., Demirçalı, A., Karcı, F., Bayrakdar, A., Taşlı, P.T., Kart, H.H., 2016. New coumarinbased disperse disazo dyes: synthesis, spectroscopic properties and theoretical calculations. J. Mol. Liq. 223, 557–565. https://doi.org/10.1016/j.molliq.2016.08.008.

Zertal, A., Sehili, T., Boule, P., 2001. Photochemical behaviour of 4-chloro-2-methylphenoxyacetic acid: influence of pH and irradiation wavelength. J. Photochem. Photobiol., A 146, 37–48. https://doi.org/10.1016/S1010-6030(01)00534-2.

Zhang, J., Nosaka, Y., 2013. Quantitative detection of OH radicals for investigating the reaction mechanism of various visible-light TiO_2 photocatalysts in aqueous suspension. J. Phys. Chem. C 117, 1383–1391. https://doi.org/10.1021/jp3105166.

Zhao, B.X., Li, X., Li, W.J., Yang, L., Li, J.C., Xia, W.X., Zhou, L., Wang, F., Zhao, C.L., 2015. Degradation of trichloroacetic acid by an efficient Fenton/UV/TiO_2 hybrid process and investigation of synergetic effect. Chem. Eng. J. 273, 527–533. https://doi.org/10.1016/j.cej.2015.03.012.

Zhou, J., Xiao, J.H., Xiao, D.X., Guo, Y.G., Fang, C.L., Lou, X.Y., Wang, Z.H., Liu, J.S., 2015. Transformations of chloro and nitro groups during the peroxymonosulfatebased oxidation of 4-chloro-2-nitrophenol. Chemosphere 134, 446–451. https://doi.org/10.1016/j.chemosphere.2015.05.027.